

Inverse modeling of nanoindentation tests to identify Ti-555 behavior

Anne-Françoise Gerday¹, Nicolas Clement², Pascal Jacques², Thomas Pardoën² and Anne-Marie Habraken¹

¹ArGenCo department, MS²F division, University of Liege, 4000 Liege, Belgium

²IMAP Department, Université Catholique de Louvain-La-Neuve (UCL), 1348 Louvain-La-Neuve, Belgium

Nanoindentation is commonly used to probe local plastic properties of materials [1-4]. From these nanoindentation tests, finite element (FE) modeling is currently used to identify material data. The general ambition of this research is to extract the material parameters representative of the response of a new generation of Ti alloy, called Ti-555, in order to perform simulations on representative microscopic cells and guide the optimization of the alloy. In this paper, the identification of the flow parameters of the β -phase of this alloy, using a microscopic crystal plasticity-based constitutive law is described. The nanoindentation tests are performed using a pyramidal Berkovich diamond indenter and the different slip systems of the b.c.c. β -phase are supposed to be activated with identical critical shear stresses. The FE nanoindentation force-displacement curves obtained with the microscopic constitutive law are compared to the experimental ones. The influence of the orientation of the grains is also analysed. A previous sensitivity analysis on different parameters with different constitutive laws and materials has shown a great influence of different parameters on the nanoindentation results but almost no influence of other parameters [5-6].

Keywords: Ti-555, finite element (FE), nanoindentation

1. Introduction

In this study, nanoindentation tests are used for material characterization. They allow the identification of basic properties, for a chosen phase, from small samples of material.

This technique is used here to extract the material parameters representative of the response of a new generation of Ti-alloy, called Ti-555 (Ti-5Al-5Mo-5V-3Cr-0.3Fe). Actually, this alloy is studied to perform fasteners [7] and should be suitable for aeronautical applications.

Ti-555 is a two phases alloy with, in general, a b.c.c. β -phase and an hexagonal α -phase. The morphology and distribution of these two phases are dictated by the thermal treatments imposed to the material. In the following sections, only the β -phase is taken into account (as the β phase is always the main constituent in this alloy, and a 100% β material can even be obtained). The grains of this phase are large enough to allow an indentation in one of these grains without problem of grain boundary effect in the response. After each experimental indentation, the indented grain is located and its orientation is measured.

In the next section, the experimental procedure of macroscopic tensile tests on the β -Ti-555 alloy, used to determine the macroscopic material parameters, and the microscopic nanoindentation tests in the β -phase of this alloy are presented. These experimental tests are performed at the IMAP department of the UCL.

The numerical approach is presented. The experiments are modeled using the *Lagamine* FE code [8] developed at the ArGenCo department, division MS²F, of the University of Liege. In order to identify the material, an elasto-viscoplastic (EVP) microscopic crystal plasticity-based constitutive law written for the FE code *Abaqus* and implemented in the FE code *Lagamine* is used. This constitutive law is briefly described and the meshes used

to model the FE tensile and nanoindentation tests are presented.

To simulate the nanoindentation tests, the parameters of the constitutive law have to be determined. To optimize these parameters for the β -phase of Ti-555, inverse modeling is performed on macroscopic tensile tests on the treated (100 % β) material. Then, the values obtained are used in the nanoindentation modeling.

The different results obtained with the simulations are presented and compared with the experimental ones. The influence of the orientation of the β -grain on the load-displacement curves is exposed.

The influence of different parameters on the results of nanoindentation simulations is commented.

2. Experimental procedure

2.1 Nanoindentation tests

Since nanoindentation simulations and tests focus on the β -phase behavior, a β -rich microstructure is chosen. This microstructure was obtained by a heat treatment close to the β transus followed by a water quench. The samples for nanoindentation are mechanically grinded using SiC papers down to 1200 and then, polished to 1 μ m with diamond paste. Finally, a mechanical/chemical polishing step is carried out with an OPS colloidal suspension during 2 hours to remove the mechanically altered surface and slightly reveal the microstructure by a gentle etching.

Nanoindentation tests are performed on a Hysitron Triboscope mounted on a Park autoprobe cp AFM-STM apparatus. A three-sided Berkovich diamond tip (figure 1) is used with a total included angle of 142.3 degrees and a half angle of 65.35 degrees.

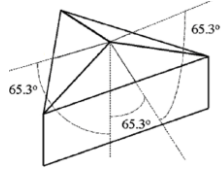


Figure 1. Berkovich diamond tip. Geometrical descriptions.

The STM mode is chosen for imaging, and nanoindentation uses the capacitive transducer to record loads up to 25 mN and depths up to 400 nm following the tip calibration on a fused silica reference sample. A load-displacement curve is then obtained for each indent. In figure 2, the experimental load-displacement curve of a 1500 μN nanoindentation test in a β grain of Ti-555 is presented.

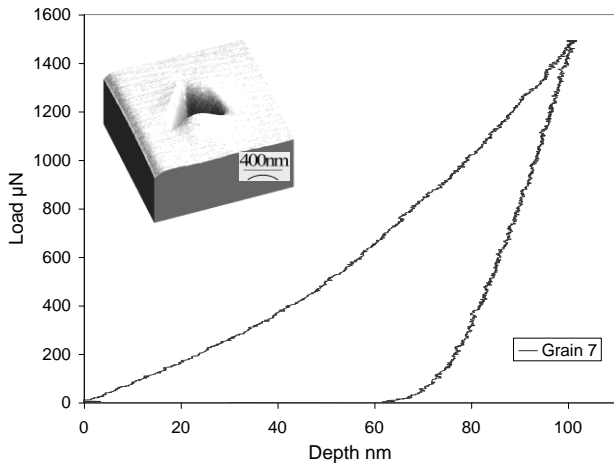


Figure 2. Nanoindentation test: load-displacement curve in a β grain of Ti-555. The grain indented is the 7th, in figure 3 with its orientation given in table 1.

This indentation was performed in the 7th grain, in figure 3. On this figure, a small part of the material, containing some β grains, is represented. For each grain, the orientation is measured and then, can be used in the modeling.

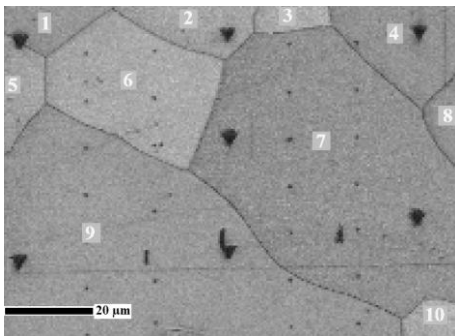


Figure 3. OIM (orientation imaging map) of the grains indented. Grains identification.

The orientations of the grains represented in figure 3 are given in table 1 by their Euler's angles (ϕ_1 , ϕ , ϕ_2).

Table 1. Orientation of the grains illustrated in figure 3

| The grain's number | ϕ_1 [°] | ϕ [°] | ϕ_2 [°] |
|--------------------|--------------|------------|--------------|
| 1 | 232.69 | 39.16 | 22.43 |
| 2 | 37.89 | 32.53 | 56.27 |
| 3 | 37.68 | 34.5 | 71.26 |
| 4 | 89.59 | 39.34 | 86.67 |
| 5 | 51.75 | 41.29 | 60.66 |
| 6 | 207.75 | 43.16 | 65.16 |
| 7 | 247.87 | 39.3 | 34.85 |
| 8 | 147.45 | 44.78 | 78.28 |
| 9 | 203.77 | 35.16 | 83.83 |

2.2 Tensile test

Experimental tensile tests have been performed for the Ti-555 aged 30 minutes at 875°C (figure 4). The thermal treatment imposed to the material leads to a 100% β -phase material at room temperature. The experimental test was performed at a strain rate of 10^{-5} s^{-1} .

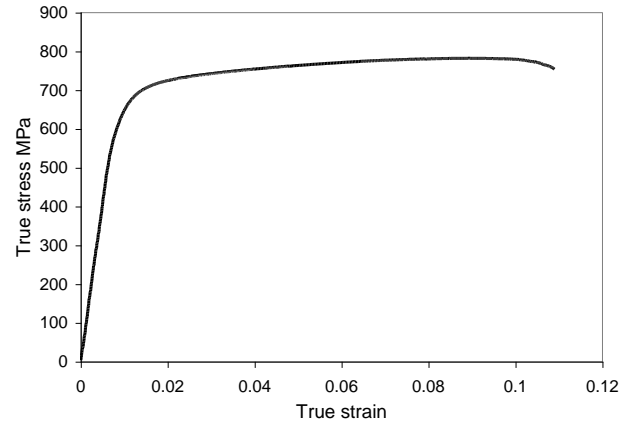


Figure 4. Tensile behavior of Ti-555 aged 30 minutes at 875°C with a strain rate of 10^{-5} s^{-1} .

3. Numerical procedure

3.1 Constitutive law

For the nanoindentation tests, an EVP microscopic crystal plasticity-based constitutive law written by Y. Huang and modified by Kysar [9] is used. In this kind of constitutive law, the crystal orientation and the activated slip systems are taken into account. Based on the Schmid law, the slipping rate $\dot{\gamma}^{(\alpha)}$ of the α^{th} slip system in a rate-dependent crystalline solid is determined by the corresponding resolved shear stress $\tau^{(\alpha)}$ as

$$\dot{\gamma}^{(\alpha)} = \dot{a}^{(\alpha)} \left(\frac{\tau^{(\alpha)}}{g^{(\alpha)}} \right)^n \quad (1)$$

where $\dot{a}^{(\alpha)}$ is the reference strain rate on slip system α , $g^{(\alpha)}$ is a variable which describes the current strength of that system, and n is linked to the strain rate sensitivity.

The strain hardening is characterized by the evolution of the strengths $g^{(\alpha)}$ through the relation :

$$\dot{g}^{(\alpha)} = \sum_{\beta} h_{\alpha\beta} \dot{\gamma}^{(\beta)} \quad (2)$$

where $h_{\alpha\beta}$ are the slip hardening moduli, the sum ranges over all activated slip systems. Here, the hardening matrix is defined by Pierce, Needleman and Asaro [9]. They assume a hyper secant relation between self- and latent-hardening moduli and overall shear strain :

$$\begin{cases} h_{\alpha\alpha} = h(\gamma) = h_0 \operatorname{sech}^2 \left| \frac{h_0 \gamma}{\tau_s - \tau_0} \right| \\ h_{\alpha\beta} = qh(\gamma) \quad (\alpha \neq \beta) \end{cases} \quad (3)$$

where h_0 is the initial hardening modulus, τ_0 is the initial value of $g(\alpha)$, τ_s is the saturation value and γ is the Taylor cumulative shear strain on all slip systems:

$$\gamma = \sum_{\alpha} \int_0^t |\dot{\gamma}^{(\alpha)}| dt \quad (4)$$

The latent hardening ratio q is taken to 1 in the next simulations. These expressions of hardening moduli neglect the Bauschinger effect in a crystalline solid.

3.2 Mesh

In order to obtain the parameters of the constitutive law for the β -phase of the Ti-555 alloy, a 3D FE mesh (figure 5) was done to model the tensile test. This mesh contains 112 eight-node brick elements [10]. To reproduce the macroscopic behavior of the material, a different orientation is given at each element and all the orientations are representative of an isotropic material.

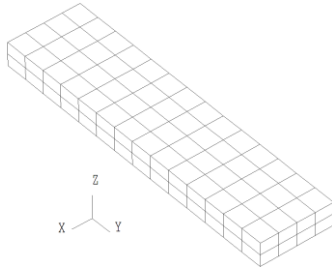


Figure 5. FE mesh used for the tensile tests.

To model the nanoindentation tests, a 3D FE mesh has been generated, refined in the contact area between the indenter and the material. It contains 1879 nodes and 1772 eight-node brick [10] elements. The mesh is partly shown in figure 6.

Contact elements [11] with 9 integration points are put in the central zone, where the mesh is refined. The indenter is considered as a rigid tool.

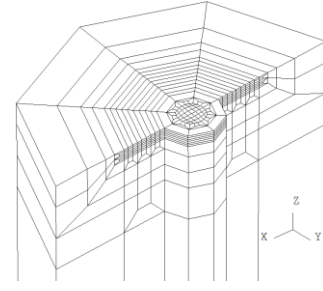


Figure 6. Part of the mesh used for nanoindentation modeling.

4. Results

4.1 Parameters of the β -phase

The elastic modulus of the β -phase is obtained from the experimental tensile test on the β -material (see table 1). A previous study has shown the small influence of the Poisson's ratio. It is taken here to 0.35. The friction coefficient is taken to $\mu = 0.2$. The value of this parameter doesn't affect significantly the load-displacement results [6] but monitors the pattern near the indented zone.

To determine the plastic parameters of the microscopic constitutive law, the inverse method is used. The program *Optim* of the FE code *Lagamine* based on the Levenberg Marquardt algorithm [12-13] determines the best parameters of the constitutive law to obtain FE tensile results as close as possible of the experimental corresponding ones. In this optimization, the different plastic parameters have the same value for each slip system (imposed). The mesh of figure 5 with random orientations of the grains is used.

The parameters obtained, given in table 2, correctly model the experimental behavior (figure 7).

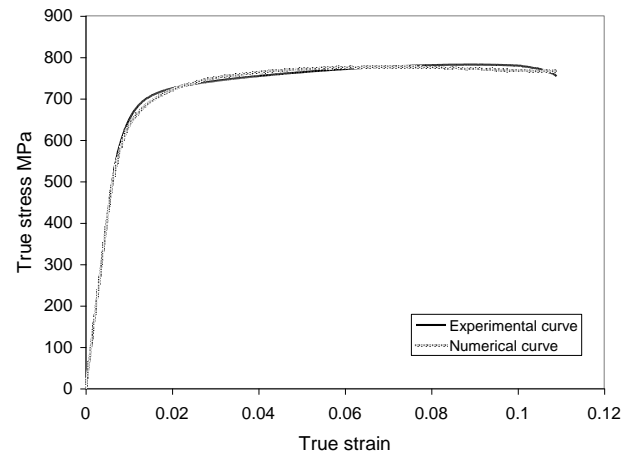


Figure 7. Tensile behavior of Ti-555 aged 30 minutes at 875°C with a strain rate of 10^{-5} s^{-1} . Experimental results and numerical ones with the parameters of table 2.

Table 2. Optimized parameters for the β -phase of Ti-555

| Elastic parameters | Parameters of the slipping rate | Parameters of the hardening |
|-------------------------|--|-----------------------------|
| $E = 85000 \text{ MPa}$ | $\dot{\alpha} = 0.0001 \text{ s}^{-1}$ | $h_0 = 13120 \text{ MPa}$ |
| $\nu = 0.35$ | $n = 19.3$ | $\tau_0 = 300 \text{ MPa}$ |
| | | $\tau_s = 353 \text{ MPa}$ |

4.2 Nanoindentation results

Two numerical nanoindentation tests were performed using the optimized parameters of table 2. The grains indented in the simulations have the same orientation as the 6th and the 7th ones of table 1. The displacement is imposed during the test.

The load-displacement curves obtained numerically with the mesh of figure 6 are compared to the experimental corresponding one in figure 8.

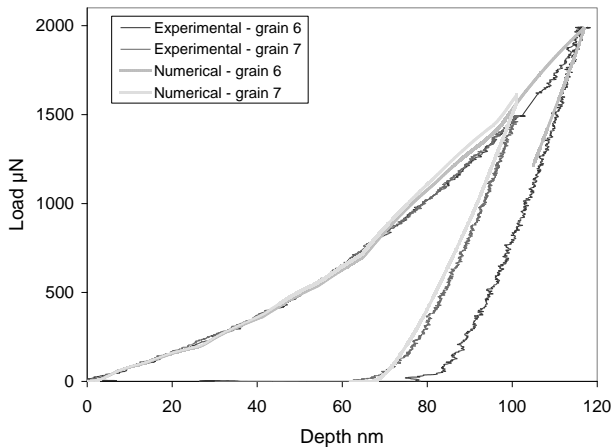


Figure 8. Experimental and numerical load – displacement curve for an indentation test on grains 6 and 7 of table 1.

At the beginning, the simulations are very close to the experimental tests. For deeper indentations, the simulated load-displacement curves diverge slightly from the experimental ones. Nevertheless, the difference between the curves is always less than 11 %.

The results are also very similar for both grains.

4.2 Discussion

The method used to reproduce the behavior of the β -phase of Ti-555 lead to interesting results. It is possible to correctly simulate the experimental nanoindentation test using the parameters obtained by inverse modeling of tensile tests. The small differences observed between the numerical and the experimental curves could come from experimental inaccuracy, limitations of the constitutive law, non perfect mesh, ...

It was also observed in experimental and numerical tests that, unlike other materials as copper (f.c.c.), the load-displacement curves seem to be independent on the orientation of the indented grain. It is probably due to the great number of symmetries and equivalent slip systems present in b.c.c. materials.

In previous studies [5-6], it was shown that nanoindentation results are highly dependent on different parameters. With a simple elasto-plastic constitutive law, changes of the elastic modulus and the plastic strength influence greatly the force-displacement results. On the other way, parameters like friction coefficient, tangent modulus or Poisson's ratio lead to very small deviations of the load-displacement curve [6]. However, the

geometry of the tip must be accurately modeled. In fact, small geometrical modifications in the definition of the indenter lead to noticeable changes in the load-displacement curves [5].

With the microscopic single crystal plasticity-based constitutive law with a conical indenter to avoid symmetries other than those of the crystal structure, it was shown for the copper that, near the indented zone, the surface of the material presents different patterns and symmetries according to the crystal orientation [5].

5. Conclusions

In this study, a method to determine the parameters of a microscopic plasticity-based constitutive law for one phase of the Ti-555 alloy was presented. The results obtained are conclusive.

In the future, the analysis of the hexagonal α -phase of the material will be studied. This part will be more sensitive because of the impossibility to obtain a material with only the α phase. The initial orientation of the grains will have probably more influence and the slip systems of an hexagonal phase are also more complicated. In this case it is necessary to use different value of the critical shear stresses for each set of slip systems.

Then, the knowledge of the characteristics of the two phases will permit to guide the optimization of the alloy by the realization of simulations on representative microscopic cells.

Acknowledgement

The authors would like to acknowledge the Walloon Region and the Belgian Science Policy through Contract PAI 5/08 and PAI 6/24 for financial support. A. M. Habraken is mandated by the National Fund for Scientific Research (Belgium).

REFERENCES

- 1) X. Chen and J.J. Vlassak : J. Mat. Res., **16** (2001) pp. 2979-2982.
- 2) R. Saha and W.D. Nix : Acta Materialia, **50** (2002) pp. 23-38.
- 3) P.L. Larsson, A.E. Giannakopoulos, E.Söderlung, D.J.Rowcliffe, R.Vestergaard : Int. J. Solids Structures, Vol. **33**, No. 2, (1996) pp. 221-248.
- 4) L.M. Farrissey, P.E. McHugh : Materials Science and Engineering A, accepted March 2005.
- 5) A.M. Habraken, A.F. Gerday, B. Diouf and L. Duchêne : "Comparisons of FEM approaches modeling the metal plastic behaviour", in *Proc. ESAFORM 2007*.
- 6) A.F. Gerday, N. Clement, P.J. Jacques, T. Pardoën, A.M. Habraken, "FE simulations of nanoindentation in beta metastable Ti", in *Proc. ESAFORM 2006*, edited by N. Juster and A. Rosochowski, Poland.
- 7) <http://asm.confex.com/asm/aero06/techprogram.htm> (paper 14136), visited in July 2006.
- 8) M. Dyduch, A.M. Habraken, S. Cescotto : JI. of Comp. Meth. in Appl. Mechanics and Engineering, **101** (1992) pp. 283-298.
- 9) Y. Huang : "A user-material subroutine incorporating single crystal plasticity in the ABAQUS finite element program", *Internal report*, (2005).
- 10) K.P. Li, S. Cescotto : Comp. Meth. In Appl. Mech. And Eng. (1997) pp. 157-204.
- 11) A.M. Habraken and S. Cescotto : Mathematical and Computer Modelling, **28**, 4-8 (1998) pp. 153-169.
- 12) K.Levenberg : Quart.Appl.Math., **2** (1944) pp.164-168.
- 13) D.W. Marquardt : J.Soc.Indust.Appl.Math., **11** (1963) pp.431-440.